Journal of the European Ceramic Society **18** (1998) 1809–1819

0955-2219/98/$—see front matter
PII: S0955-2219(98)00120-4

Oxidation Resistance of SiC/SiC Micro and Minicomposites with a Highly Crystallised BN Interphase

F. Rebillat,* A. Guette, L. Espitalier, C. Debieuvre and R. Naslain

Laboratoire des Composites Thermostructuraux, UMR 5801, CNRS-SEP-UB 1, 3 allée de la Boëtie, 33600 Pessac, France

Abstract

A three dimensionally ordered hex-BN is deposited by LPCVD from the BF_3–NH_3 system at relatively low temperature. This coating was studied in term of crystallisation by X-ray diffraction, and transmission electron microscopy. SiC/SiC microcomposites with such a BN interphase were produced in a first step. Their mechanical behaviour was determined under tensile loading at room temperature. They exhibited a wide non-linear stress–strain domain similar to that commonly observed during the damage of a ceramic matrix composite. Further, static fatigue tests at 700°C in air were carried out on a few microcomposites. The long lifetimes provide evidence that such a BN-based interphase brings a real improvement in the oxidation resistance. In a second step, from these latter results, minicomposites were prepared with a complex interphase consisting of a few layers of BN, which included a highly crystallised layer. Similar mechanical tests at room temperature and static fatigue tests at high temperature in air were performed. Despite the change of geometry (single fibre to a tow), damage capability and improved oxidation resistance are observed in comparison with minicomposites with a carbon interphase. © 1998 Elsevier Science Limited. All rights reserved

Keywords: boron nitride, microcomposite, minicomposite, tensile test, oxidation, lifetime

1 Introduction

SiC/SiC composites, as many other fibrous ceramic matrix composites (CMCs), exhibit a high toughness, with respect to monolithic ceramics, coupled to an extended non-linear behaviour under tensile loading, when properly processed. These properties are directly related to the occurrence of various well identified energy dissipating mechanisms, i.e. matrix microcracking, fibre/matrix debonding, fibre sliding and fibre extraction.[1,2] However, it is now well established that the onset of these energy dissipating mechanisms requires a low enough shear strength interface between the fibres and the matrix.[3] This requirement is usually achieved through the use of an interfacial compliant material, referred to as the interphase. So far, materials with a layered crystal structure such as pyrolytic carbon have been the most widely used interphases.[4,5]

Boron nitride has been suggested as an alternative to anisotropic pyrocarbon in various CMCs for service at elevated temperatures in oxidising atmospheres.[6,7] There is indeed a marked structural similarity between hexagonal BN and graphite.[8] Further, BN displays an unusual combination of properties including thermal stability, corrosion resistance and mechanical properties.[9,10]

The aim of this work was to obtain thin coatings of Pyro-BN by low pressure chemical vapour deposition (LPCVD) on SiC fibres with a controlled structure and microtexture in order to achieve: (i) a range of thermal and mechanical characteristics, and (ii) corrosion and oxidation resistance at relatively high temperatures, better than that previously reported for pyrolytic carbon interphases.

2 Experimental Procedure

2.1 Samples

2.1.1 Model composites

In this study, two kinds of samples are used and considered as elementary cells of a real composite: micro- and minicomposites.

Microcomposites consist of concentric cylindrical specimens obtained by coating a single fibre

---

*To whom correspondence should be addressed.

with an interfacial material and a matrix. For their fabrication, the fibres were extracted from a bundle and the single filaments fixed straight on a graphite frame. The frames were set in the hot zone of the CVD reactor to receive BN coatings. The SiC/BN/SiC microcomposites investigated in the present paper are made of Nicalon fibres (15 μm diameter), a boron nitride interphase (0·8 μm thick) and a SiC matrix deposited by CVD (2 μm thick). Their constituents are representative of their counterparts in the actual composites, since: (i) they are produced using identical chemical vapour deposition conditions,[11] and (ii) the volumetric ratios of the constituents are maintained.

The minicomposites consist of a tow (composed of around 500 monofilaments). The interphase and the matrix are elaborated as carefully as previously mentioned. Their geometry is closer to that of a composite. Their processing is done following a similar procedure, described above, by fixing tows straight on a frame before their introduction in the CVD reactor.

2.1.2 Fibres

Two kinds of SiC fibres (from Nippon Carbon) are used after being desized: Nicalon NLM 202 and Hi-Nicalon fibres, for microcomposites and minicomposites. The NLM 202 contains a relatively high quantity of oxygen (>10 atom%) and can be considered as Si–C–O fibres. Its surface composition is close to silica.[12,13] In contrast, the Hi-Nicalon has a reduced concentration of oxygen (<5 atom%) and a C/Si ratio equal to $\approx 1{\cdot}4$. A carbon-rich layer covers this fibre surface.[14,15]

2.1.3 Preparation of BN interphases

In common low pressure CVD (LPCVD) processing conditions, boron nitride is often poorly crystallised. Heat treatments at very high temperatures (beyond 2000°C) are required to obtain hexagonal boron nitride.[16,17] The apparatus used in this study has been described elsewhere.[18] BN deposition was carried out in a hot-wall, LPCVD-reactor, from the BF_3–NH_3–Ar or BCl_3–NH_3–H_2 gaseous system on fibrous substrates. The BF_3–NH_3–Ar system is preferred to deposit crystallised BN with a controlled texture, and BCl_3–NH_3–H_2 for lower processing temperatures which limits fibre/gaseous phase reactions and strengthens the fibre/BN interfacial bond. The bases for the choice of these conditions were given elsewhere.[11,19]

In a system with NLM 202 Nicalon fibres, the fibre/BN interface often constitutes the weakest bond in the interfacial sequence.[12,13]

In the BF_3–NH_3–Ar gaseous precursor system, silicon is eliminated as SiF_4 gaseous species:[12]

$$3SiC_{(s)} + 4BF_{3(g)} \rightarrow 3SiF_{4(g)} + 4B_{(s)} + 3C_{(s)}$$

$$\begin{aligned} 4BF_{3(g)} + n''Si_xC_yO_{z(s)}'' \rightarrow\, & 3SiF_{4(g)} \\ & + ''B_4Si_{(nx-3)}C_{ny-m}O_{nz}'' \\ & + mC \end{aligned}$$

As a result, a carbon layer, containing boron, is formed. It constitutes the weak bond in the interfacial sequence. To limit this gas/fibre surface chemical reaction, the BCl_3–NH_3–H_2 system is preferred to deposit the first BN layer against the fibre.

However, with High-Nicalon fibres containing less oxygen,[14,15] the reaction with the gaseous phase is limited during the process, and so a stronger fibre/BN coating bond can be obtained.

2.2 Chemical characterisation

X-ray diffraction patterns were recorded using D-5000 equipment from Siemens and Cu K_α radiation ($\lambda = 1{\cdot}54$ Å). X-ray diffraction was used to assess the BN crystallisation state and to detect the preferred orientations of the (002) planes against the substrate surface. Pole figures were recorded from BN films deposited on planar substrates. A pole figure is obtained by recording, through a stereographic projection, the intensity diffracted by a (hkl) plane when the sample is tilted in all possible orientations in space. The points of iso-intensity, on this projection, are linked by contour lines to form the pole figure. The point with the maximal intensity gives the space direction in which the maximum of the (hkl) planes are stacked. It can also be drawn a three dimensional representation of these data (using TEX-AT software from SOCABIM).

The matrix cracking and failure surface of the model composites was characterised by scanning electron microscopy (SEM: Hitachi 400). The microstructure and texture of BN coatings were studied by transmission electron microscopy (TEM: CM 30 Philips).

The debonded fibre surface compositions along pull-out lengths after mechanical tests on these composites were analysed by Auger Electron Spectroscopy (AES: Microlab from Vacuum Generators) coupled with argon-ion etching. The analysis of the respective atomic percentage of each element (B, C, N, O, Si) was performed close to fibre surfaces and in depth profiling.

2.3 Mechanical tests

2.3.1 Tensile tests at room temperature

The tensile tests on microcomposites used a specific table-model testing machine initially designed and developed for fibre testing.[20] An accurate measurement of their diameters was made with a laser diffraction system. The microcomposites were tested according to the single fibre tensile test procedure.[21,22] Their very simple geometry allows an easy characterisation of the interphase and the extraction of its intrinsic mechanical properties.[23]

From the stress–strain tensile curves, the failure stress and strain, and the Young's modulus were directly extracted. The data were statistically analysed by means of the two parameter Weibull distribution: the failure stress at 50% chance of survival ($\sigma^{R}{}_{(50\%)}$), and the Weibull modulus (m).[24,25] This method allows to check by variation of these two Weibull parameters that the corrosion of the fibres, during the process, leads to the modification of the population of the surface defects with an alteration of the failure properties.

The minicomposites are closer to the arrangement of fibres in a composite. Their tests were done on a specially built system.[26] By considering a minicomposite as a sum of microcomposites (500 single filaments), a similar analysis of their mechanical behaviour[23] can be performed. The estimation of the sections, i.e. the surface area of the failure facies, can be done by image analysis or weighing the samples. These methods are not very accurate. In particular, since in a minicomposite, the fibres do not break simultaneously but progressively with the raising applied load, it is preferred to give, as a failure characteristic, a failure load rather than a failure stress. For comparison between mechanical characteristics of microcomposites and minicomposites, failure stresses for minicomposites are calculated by carrying the ultimate load over to the total section.

2.3.2 Lifetime at high temperature under tensile loading

The specimen was vertically maintained in the heating area under air, following the procedure described by Jacques *et al.*[27] for microcomposites and by G. A. Lebrun *et al.*[26] for minicomposites. The stress (respectively, 600 MPa for the microcomposites and 60 N for the minicomposites) was chosen up to the cracking stress of the matrix identified in the stress–strain curves previously established at room temperature. For a temperature of 700°C, the lifetime (i.e. the time before failure) of each specimen was measured.

3 Results and Discussion

3.1 NLM 202 Nicalon fibre/BN(ex-BF_3)/SiC microcomposites

3.1.1 Structural analyses of BN coatings

The scanning electron microscopy shows a deposit with faceted columnar grains with sharp edges around flat-topped surfaces [Fig. 1(a)]. The diameter of these columns is estimated to be about 1 μm. An XRD study, using the method of pole figures [Fig. 1(b)], highlights a pronounced preferential direction of growth of the (002) planes perpendicular to the substrate surface. The small width of the peak is related to a limited disorder in the stacking of (002) planes.

The interfacial fibre/coating zone and the BN interphase anisotropy perpendicular to the fibre surface (degree of crystallisation and microtexture) were studied by transmission electron microscopy on transverse cross-sections. As seen in Fig. 2(a), this BN grows with a columnar grain texture. In each column, all the (002) planes are parallel to each other and to the fibre surface [Fig. 2(b)]. Furthermore, the selected area diffraction (SAD) pattern evidenced the very high ordering of atomic planes [Fig. 2(c)].

Such a textured BN coating should possess the required mechanical and thermal properties to be used as an interphase.

3.1.2 Mechanical behaviour of SiC/BN/SiC microcomposites

3.1.2.1 Tensile test at room temperature. The microcomposites exhibit a non-linear stress–strain

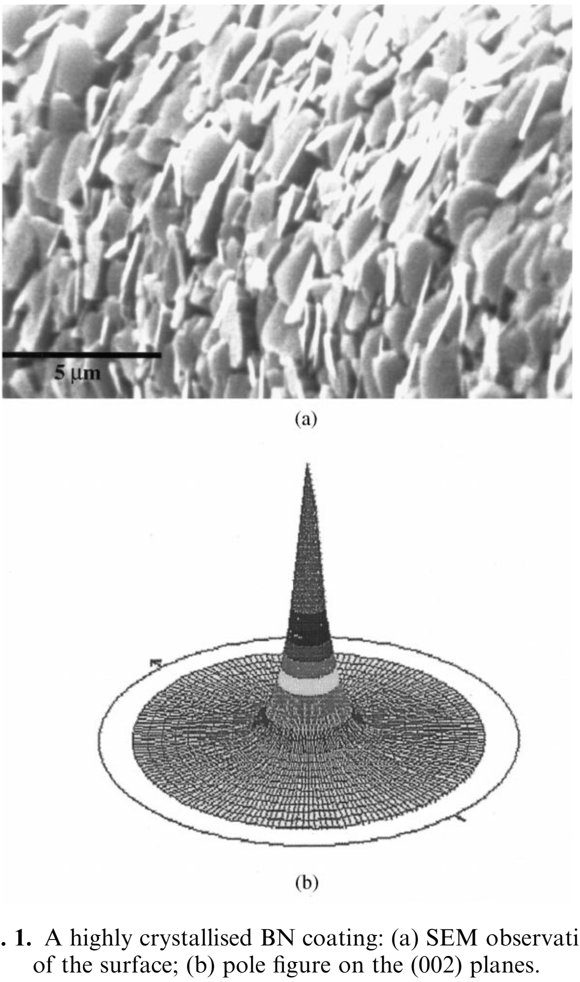

Fig. 1. A highly crystallised BN coating: (a) SEM observation of the surface; (b) pole figure on the (002) planes.

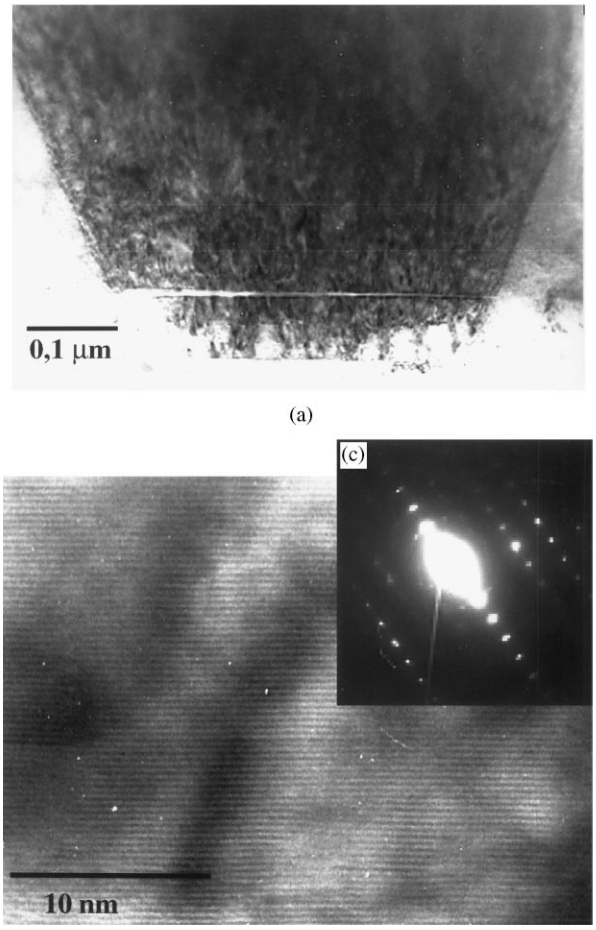

(a)

(b)

Fig. 2. TEM observations of a highly ordered BN coating: (a) columns of growth; (b) (002) planes; (c) SAD pattern.

behaviour extending over a wide range of deformation, and rather large strains to failure (up to 1%, Fig. 3). A clear plateau-like feature was observed, suggesting the presence of relatively weak fibre/matrix interactions, a low density of matrix cracks at saturation and evidence for long debonded lengths. The failure characteristics are high: $\sigma^R = 1400\,\mathrm{MPa}$ and $\varepsilon^R = 1{\cdot}1\%$. The initial Young modulus of the undamaged microcomposite close to that of the fibre, due to the presence of a thick BN interphase ($V_{\mathrm{fibre}} = 50\%$, $V_{\mathrm{BN}} = 15\%$ and $V_{\mathrm{matrix}} = 35\%$).

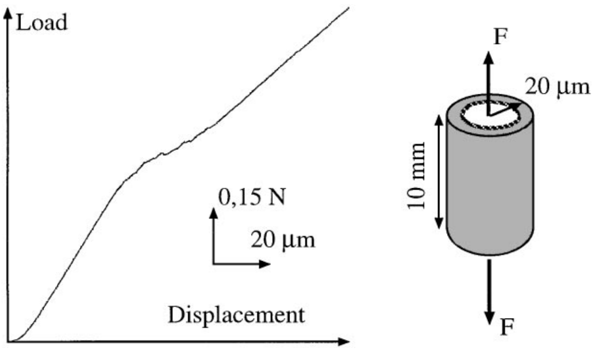

Fig. 3. Tensile test at room temperature for a SiC/BN/SiC microcomposite.

Finally, the microcomposites exhibited stress/strain curves very similar to those commonly obtained for the 2D composites.[28] The weak fibre/BN interface seems to control the localisation of debonding in the interfacial sequence.

3.1.2.2 Lifetime at high temperature. Figure 4 shows that the BN interphase displays a better oxidation resistance than its pyrolytic C counterpart since a less marked decrease of the percentage of unbroken microcomposites with time is observed. The scanning electron microscopy (SEM) observations (Fig. 5) showed that: (i) close to a matrix crack the whole BN coating is replaced by a glass probably rich in B_2O_3 and (ii) farther from a matrix crack, a BN coating is always present along the matrix side but replaced by a porous oxide along the fibre surface.

Since debonding occurs at the fibre/BN interface, the oxidation of the interphase certainly begins along the debond length, on the fibre side. Moreover, close to the fibre, BN is also observed to be less crystallised [lower degree of crystallisation and smaller grain size, as evidenced in Fig. 2(a)] and so, it has a lower oxidation resistance than BN close to the matrix.

3.2 Microcomposites with Hi-Nicalon fibre and tailored BN interphase

The introduction of Hi-Nicalon fibres in SiC/BN/SiC composites has two goals: (i) a better chemical compatibility between the fibres and the BN gaseous precursors and consequently between the fibres and the BN coatings, and (ii) an improvement of failure properties of these composites.

To get a better control of formation of the fibre/BN interface, it is required to find fibres with a more chemically stable surface than the Si–C–O NLM 202 Nicalon fibres.[12] The silica layer, initially present at the fibre surface, which thickens during the coating process, is often the weakest bond in the fibre/matrix interfacial sequence.[12,13] A preferential debonding, at one of the interfaces along this silica layer, then occurs instead of a deviation and propagation of matrix cracks inside the interphase. Such a localisation of the debonding prevents the interphase from playing its role as a mechanical fuse. The SiC fibre (Hi-Nicalon) with a low oxygen content, now available, was chosen in the remaining work. In the absence of this SiO_2 layer, the weakest bond in the interfacial sequence is expected to be inside the interphase.

In order to reduce the corrosion of the fibre surface and so to strengthen the fibre/BN bond, a first BN coating on the fibre was prepared from the (BCl_3, NH_3) gaseous precursor phase. This BN(ex-BCl_3) layer is expected to play the role of a diffusion barrier against the BF_3 gas used to deposit a highly crystallised BN(ex-BF_3) coating.

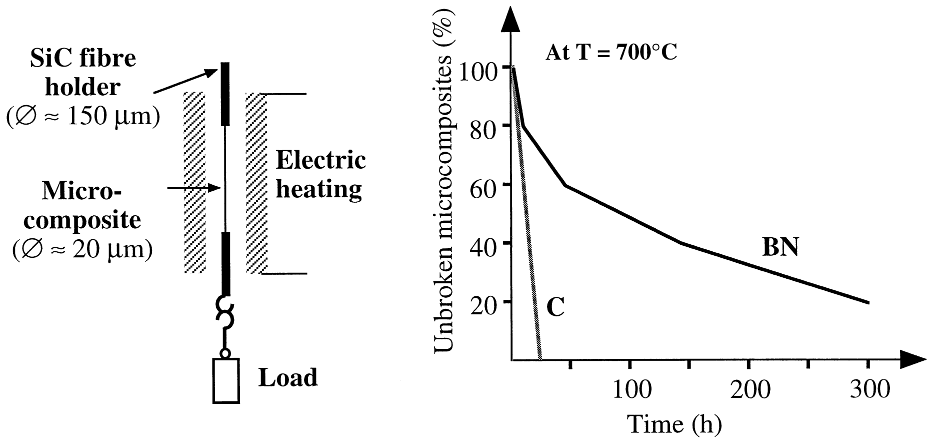

(a) (b)

Fig. 4. Static fatigue for SiC/SiC micro-composites with BN or C interphases at high temperature: (a) mechanical test system; (b) evolution versus time of percentage of unfailed microcomposites.

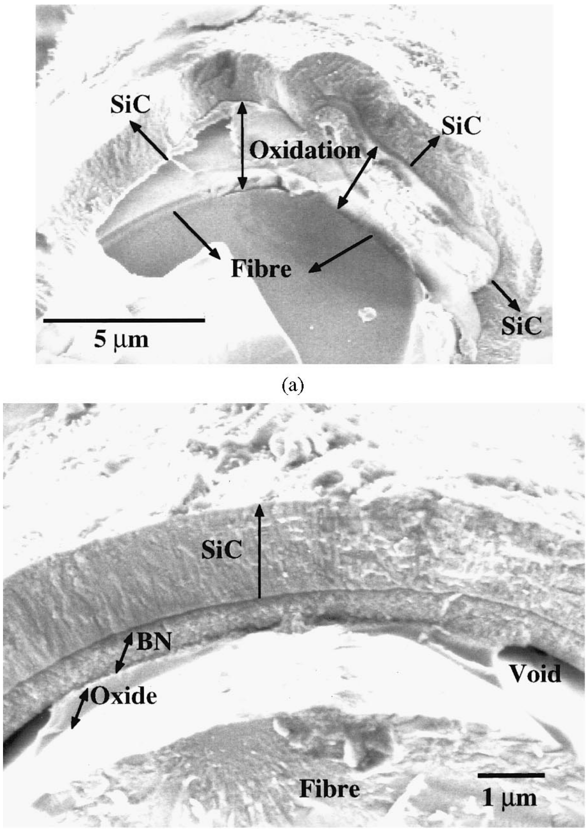

(a)

(b)

Fig. 5. SEM observations of an interfacial zone of a SiC/BN/SiC microcomposite after 3 weeks of oxidation: (a) close to a matrix crack; (b) further from a matrix crack.

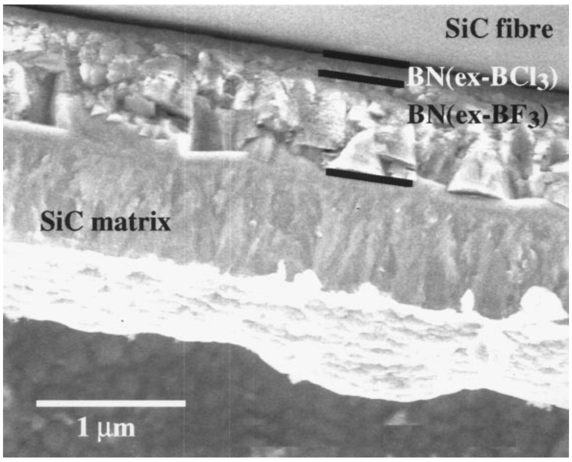

Fig. 6. Observation by SEM of the layered BN interphase.

For the first time, microcomposites with a bi-layered interphase, BN(ex-BCl_3) and BN(ex-BF_3), were prepared (Fig. 6). The whole interphase thickness is around 0·5–0·7 μm. An Auger Electron Spectroscopy analysis across this interphase showed that no difference in composition exists between the two successive layers: (1) BN(ex-BCl_3) and (2) BN(ex-BF_3). The curves from tensile tests on these microcomposites exhibit a large non-linear domain [Fig. 7(a)]; the failure characteristics, assuming the load was applied to the whole section of the microcomposite, are the following: $\sigma^R_{(50\%)} = 2450$ MPa and $\varepsilon^R = 1{\cdot}2\%$. In parallel, a matrix multi-cracking is observed by scanning electron microscopy [Fig. 7(b)]. Close to the failure, the fibres only are loaded (linear part); the load transfer is complete from the matrix to the fibre. It seems that the fibres are not corroded by the BN gaseous precursors during the BN CVD process since: (i) the failure properties of the fibres inside the microcomposites (calculation of σ^R by carrying the load applied over to the only fibre section) are similar to those of the initial fibres:

- $\sigma^R_{(50\%)} = 2960$ MPa and $m = 8{\cdot}8$, for the initial High Nicalon fibres used,
- $\sigma^R_{(50\%)} = 2900$ MPa and $m = 7$, for the fibres inside the microcomposites, and
- (ii) the defects initiating the fibre failure remain in the volume.

Following these promising results, minicomposites with such an interphase were made to get specimens closer to the composite morphology.

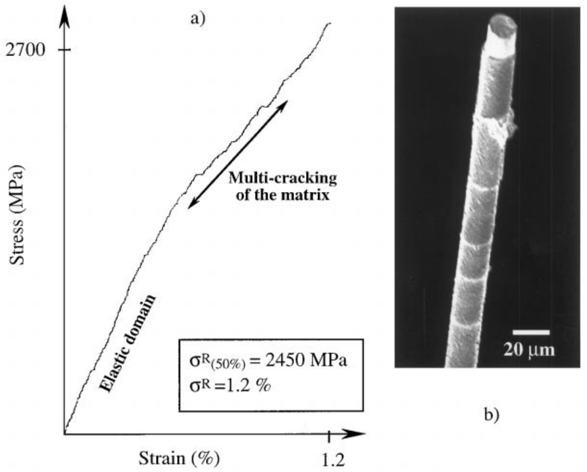

Fig. 7. Tensile test on a SiC/SiC microcomposite with a layered BN interphase: (a) stress–strain curve; (b) SEM micrograph of a broken microcomposite showing the matrix cracks.

3.3 Hi-Nicalon fibre/BN(ex-BCl_3)/BN(ex-BF_3)/ SiC minicomposites

The minicomposite is a preferred representation of the unit cell of a composite, because the stress field in a bundle takes into account the interactions between the neighbouring fibres. The mechanical behaviour of a minicomposite remains simple to interpret, since it has a unidirectional orientation of the fibres and each matrix crack can be supposed to completely cross the bundle from one side to the other, creating a similar interfacial damage around each fibre.[23,26] However, the transition from microcomposites to minicomposites is not simple, mainly due to the differences in reproducibility of the deposition kinetics and degree of crystallisation of coatings at the surface of a single fibre and inside a bundle.

Minicomposites with a similar interphase to the microcomposites did not give the expected results (Fig. 8). Their behaviour was brittle, highlighting a very strong fibre/BN bond and a not weak enough cohesion inside the interphase. In the guest to strengthen the interfacial bond, a different multilayering of the BN interphase was chosen to weaken the latter. An interphase with a gradation of structure was realised, consisting of a BN multilayer composed of: (i) a coating against the fibre made of a BN(ex-BCl_3), and (ii) a succession of three BN(ex-BF_3) layers with a degree of crystallisation decreasing from the fibre to the matrix. Such an interfacial concept with a gradation of crystallisation has been introduced by Jacques,[29,30] [in C(B) interphases with the concentration of boron increasing from the fibre to the matrix].

Thus, the crack coming from the matrix is expected to be deviated progressively from the mode I to the mode II across the interphase and to propagate inside the most crystallised layer, without reaching the fibre surface protected by the BN(ex-BCl_3) layer (Fig. 9).

3.4 Mechanical behaviour of minicomposites with a crystallisation-graded BN interphase

3.4.1 Tensile test at room temperature on minicomposites with a crystallisation-graded BN interphase

The stress–strain curves from the tensile tests exhibit a large non-linear behaviour, characteristic of a wide damage in composites with a weak interfacial bond (Fig. 10). In the same way, the hysteresis loops are wide and the residual strains for a complete

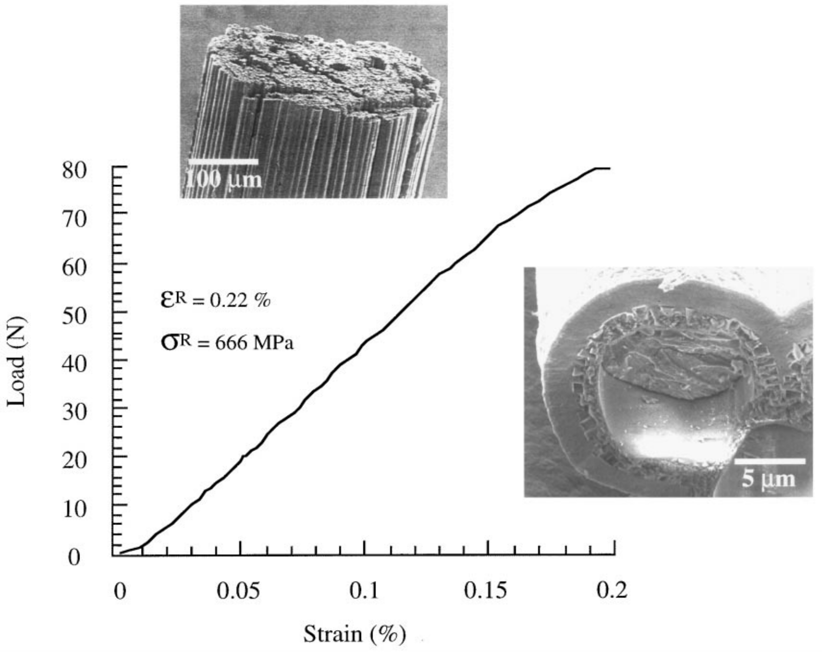

Fig. 8. Tensile behaviour of a SiC/SiC minicomposite with a bi-layer BN interphase.

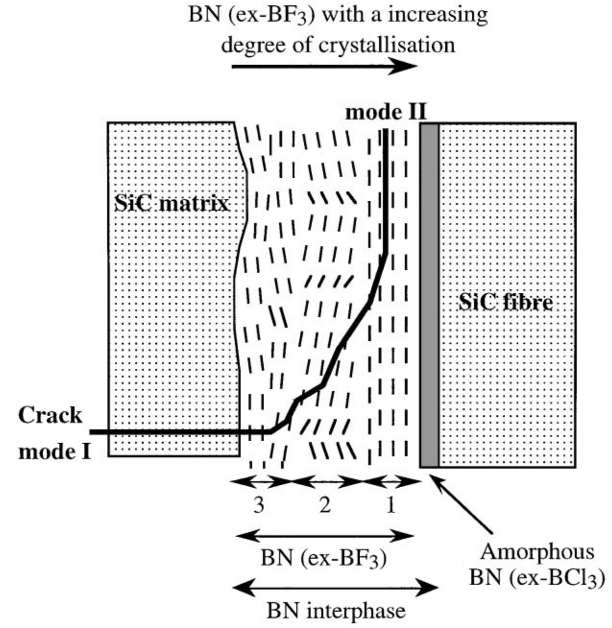

Fig. 9. Predicted deviation of a matrix crack from mode I to mode II in a graded crystallisation BN interphase of a SiC/SiC minicomposite.

unloading are significant. The matrix is highly cracked, and relatively long pull-out lengths ($>20\,\mu$m) are observed, as shown on Fig. 10. From accurate scanning electron microscopy (SEM) observations, a layer always appears to cover the extracted fibre surface [Fig. 11(a)]. It was identified as BN by Auger Electron Spectroscopy. The first BN(ex-BCl$_3$) coating appears to remain bonded to the fibre surface. However, this first BN coating does not have a uniform thickness around the fibres [previously checked during the BN(ex-BCl$_3$) process] and can sometimes not continuously cover the fibre. From these observations, the cracks seem to be deviated inside the BN interphase and to

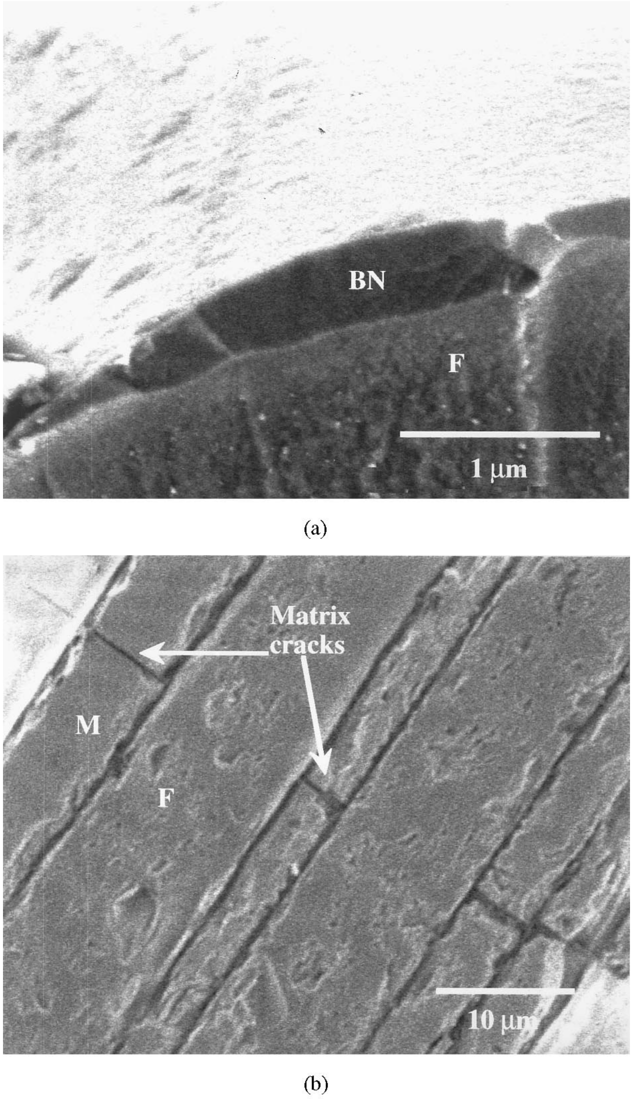

(a)

(b)

Fig. 11. SEM observation of the matrix crack deviation in a graded crystallisation BN interphase after a tensile test on a SiC/SiC minicomposite: (a) fibre side; (b) transverse polished surface.

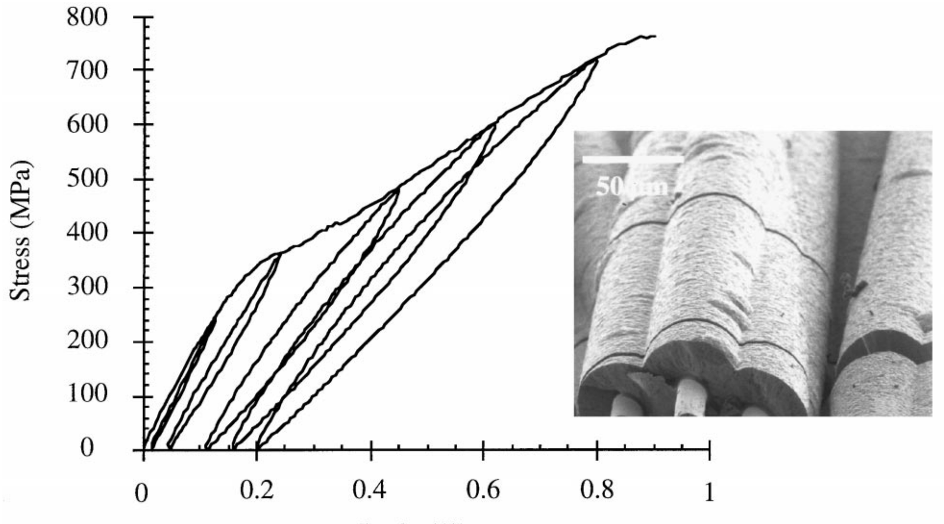

Fig. 10. Tensile test on a SiC/SiC minicomposite with a graded crystallisation BN interphase.

propagate in mode II at the interface of BN(ex(BCl_3)/BN(ex-BF_3) (highly crystallised) layers [Fig. 11(b)]. This deviation of cracks is close to that expected previously, drawn on Fig. 9.

3.4.2 Lifetime at high temperature of minicomposites with a crystallisation-graded BN interphase

The SiC/SiC minicomposites with this crystallisation graded BN interphase display a better oxidation resistance than the minicomposites with a pyro-carbon interphase[31] with lifetimes, under static loading at 700°C, respectively equal to 18 h and less than 2 h.

The failure surface of tested SiC/BN/SiC minicomposites are characteristic of a brittle composite, with no pull-out (Fig. 12). The interphase has almost disappeared, leaving large voids around the fibres; the load transfer is no longer efficient close to this failure zone. Accurate SEM observations of extracted fibres show the presence of a glassy phase covering them uniformly. The fibre surfaces are very rough and characteristic of the solidification of a B-rich oxide glass. Surface Auger Electron Spectroscopy confirmed the formation of B_2O_3. Hence, the fibres are certainly degraded by a chemical corrosion of their surfaces by this glassy phase and/or oxygen diffusing to them. Furthermore, the defects which initiate fibre failures are observed close to the surface.

The SEM observations of the interfacial zone, far from the failure surfaces, showed the presence of a few voids around each fibre in a quite dense material (Fig. 13). This material seems mainly made of a glassy phase, electrically charging under the electron beam of the SEM. Finally, the initial BN interphase appears to be almost completely oxidised.

The isotropic BN(ex-BCl_3) coating close to the fibre is extremely sensitive to oxidation.[19,32] The consequence is a rapid formation of a glassy phase at the fibre/BN(ex-BF_3) interface, which corrodes the fibres[33] and certainly oxidises prematurely the crystallised BN(ex-BF_3) coating at relatively low temperatures through a phenomenon of dissolution.

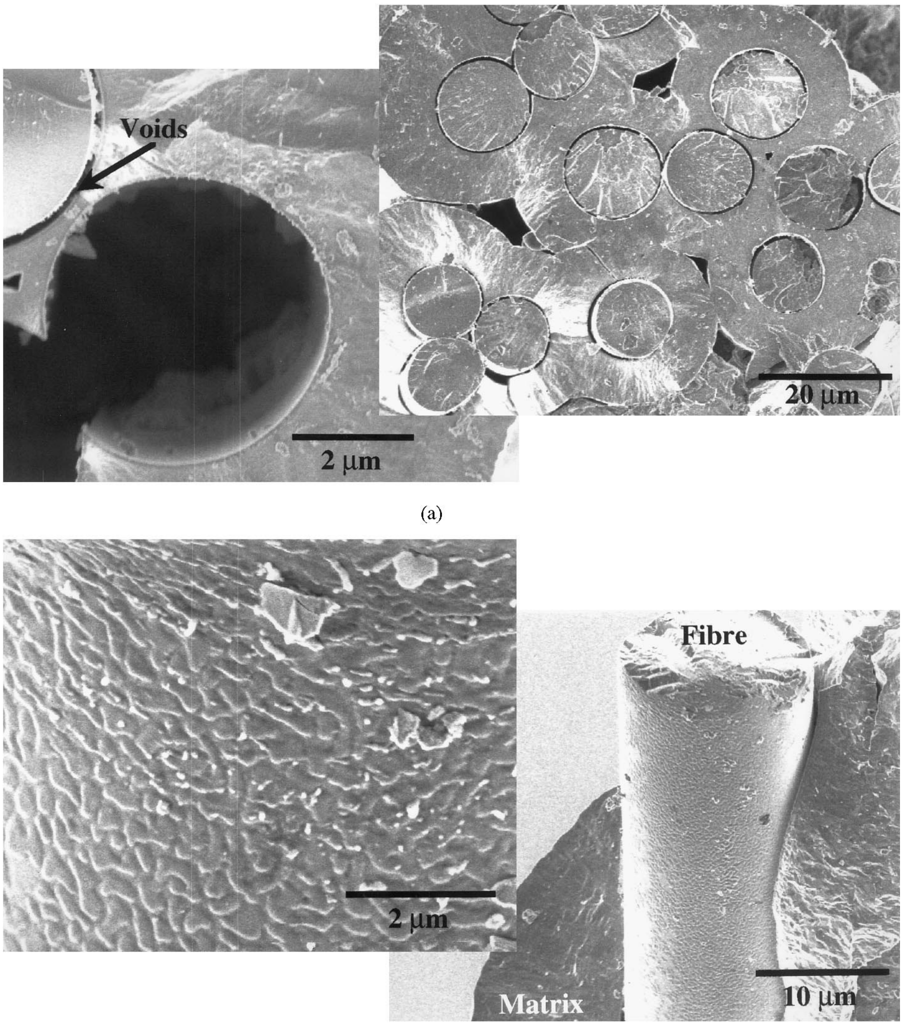

(a)

(b)

Fig. 12. SEM observations of the failure surfaces of a SiC/SiC minicomposite with a crystallisation graded BN interphase after static loading at 700° for 18 h: (a) failed fibres and interfacial zone; (b) extracted fibre surface.

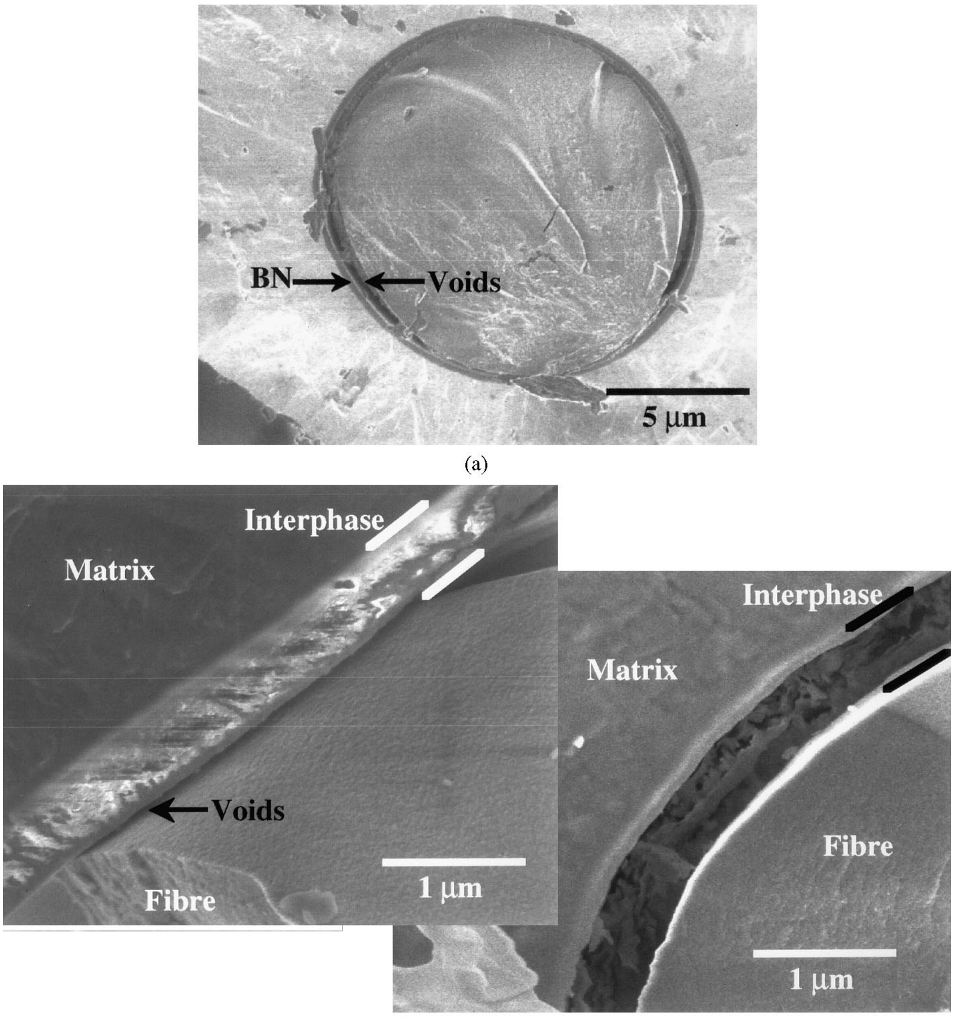

(a)

(b)

Fig. 13. SEM observations of a SiC/SiC minicomposite with a crystallisation graded BN interphase after static loading at 700°C for 18 h, far from the failure: (a) interfacial zone around a fibre; (b) fibre/matrix interfacial sequence.

Since a real improvement of lifetime is obtained by replacing the C interphase in SiC/SiC minicomposites by BN, the B_2O_3 then produced by oxidation of BN acts as a diffusion barrier against air. As long as B_2O_3 is present, this barrier remains efficient, but B_2O_3 volatilises (the interphase almost disappeared, leaving large voids around the fibres). In conditions of oxidation in pure O_2,[34] it should stay in a condensed state, and fill the space between the fibre and the matrix. The moisture in ambient air is the essential factor permitting the volatilisation of B_2O_3 at low temperature ($<$ 1000°C) and atmospheric pressure. Furthermore, even if the corrosion of the fibre by B_2O_3 is expected, it seems much less intense than that by O_2 gas. In summary, the fibres underwent two kinds of corrosion: (i) a liquid corrosion by a melted B-rich glass and (ii) a gaseous corrosion by O_2, coming toward the fibres through the matrix cracks and diffusing inside the glassy phase covering them. The O_2/fibre surface reaction and the oxidation kinetics can then increase catastrophically as soon as B_2O_3 is volatilised, in a similar manner to that in SiC/SiC with a C interphase (when C disappeared). Some calculation of reaction kinetics of corrosion and volatilisation of B_2O_3 by H_2O (in air) would allow the prediction of the time of disappearance of the B_2O_3 glass around the fibres.

4 Conclusion

The conditions for the CVD-deposition of a three-dimensional ordered BN were identified. Such BN has rarely been processed with a texture similar to that of strongly anisotropic pyrocarbon. Large columns form the coating. In each of them, the (002) planes are almost perfectly parallel over distances greater than a micrometer.

The stress/strain curves of SiC (NLM 202)/SiC microcomposites with a highly crystallised BN interphase were found similar to those recorded for other 2D composites. The oxidation resistance of this BN interphase and consequently the lifetime of the microcomposites appears to be much higher than those with a pyC interphase. This improvement is also due to the formation of a molten glass that limits the oxygen diffusion along the debonded surfaces. Thus, the kinetics of oxidation are slowed down and the load transfer between the constituents is maintained for a longer period.

SiC/SiC microcomposites with fibres with a very low O_2 ratio (Hi-Nicalon) and a tailored BN interphase [BN(ex-BCl_3)/BN(ex-BF_3)] were fabricated. With the CVD/CVI process, the fibres are not chemically degraded, and, during a tensile test, they can bear, after saturation of microcracking of the matrix, the applied load up to the failure by themselves. From these promising results, minicomposites were made.

The transition from microcomposites to minicomposites is not simple. There is not often a good reproducibility of the deposition kinetics and degree of crystallisation of coatings processed in similar conditions. Thus, the confined gaseous phase in the porous geometry of a tow causes a stronger chemical degradation of fibre surfaces. To get the required tensile behaviour at room temperature, a crystallisation graded BN interphase was developed. The debonding occurs in the interphase, close to the BN(ex-BCl_3)/BN(ex-BF_3) interface. At high temperature under static loading, close to the failure zone, the interphase almost disappeared completely, leaving an empty ring around the fibres, and so a discontinuity in the fibre/matrix interfacial sequence. The fibre surface is covered by a B-rich glassy phase. Further from the failure zone, a dense glassy phase with just a few voids replaced the BN interphase. The very low oxidation resistance of the first BN(ex-BCl_3) layer against the fibre is possibly responsible to the lowering of the whole BN interphase oxidation resistance through its quick transformation in B_2O_3. A clear improvement (around one order of magnitude) of the lifetime in air is reached by replacing the C interphase by BN. In this latter case, B_2O_3 acts as a diffusion barrier to O_2 gas, as long as it fills the fibre/matrix interfacial space. If the corrosion of fibres by B_2O_3 is expected, it seems to be less intense than that by O_2 gas.

If strengthening of the fibre/BN interface is to be achieved, an increase of the oxidation resistance of the BN(ex(BCl_3) via enhanced crystallisation is required to improve the high temperature behaviour of such SiC/BN/SiC minicomposites.

Acknowledgements

This work has been supported by the French Ministry of Education, Research and Technology, CNRS and SEP. The authors are indebted to C. Robin Brosse and S. Goujard from SEP for valuable discussions and they are grateful to M. Lahaye for the AES analyses.

References

1. Evans, A. G. and Marshall, D. B., The mechanical behavior of ceramic matrix composites. *Acta. Metall.*, 1989, **37**, 2567–2583.
2. Quenisset, J. M., Damage mechanisms in composite materials. In *23e colloque du groupe français de rhéologie, General Conference*. LMP-CEPMUB, Bordeaux, 1988, pp. 1–41.
3. Cao, H. C., Bischoff, E., Sbaizero, O., Ruhle, M., Evans, A. G., Marshall, D. B. and Brennan, J. J., Effect of interfaces and the properties of fiber-reinforced ceramics. *J. Am. Ceram. Soc.*, 1990, **73**(6), 1691–1699.
4. Naslain, R., Fiber-matrix interphases and interfaces in ceramic matrix composites processed by CVI. *Composite Interfaces*, 1993, **1**(3), 253–286.
5. Dupel, P., Bobet, J. L., Pailler, R. and Lamon, J., Influence d'interphases pyrocarbone déposées par CVI pulsée sur les caractéristiques mécaniques de matériaux composites unidirectionnels. *J. Phys. III, France*, 1995, **5**(7), 937–951.
6. Lowden, R. A. and More, R. L., The effect of fiber coating of interfacial shear strength and the mechanical behavior of ceramic composites. *Mat. Res. Symp. Proc.*, 1990, **170**, 205–214.
7. Singh, R. N. and Brun, M. R., Effect of boron nitride coating and fiber-matrix interactions. *Ceram. Eng. Sci. Proc.*, 1987, **7**(7–8), 636–643.
8. Chrétien, A., Combinaison avec l'azote et le phosphore. In *Traité de chimie minérale*, ed. P. Pascal, Vol. VI. Masson and Cie, Paris, 1961, pp. 249–256.
9. Ingles, T. A. and Popper, P., *Boron Nitride*, ed. A. T. Green, Research Paper no. 398. The British Ceramic Research Association, 1958, pp. 1–27.
10. Dana, S. S., The properties of low pressure chemical vapor deposited boron nitride thin films. *Mat. Sci. Forum*, 1990, **54** and **55**, 229–260.
11. Rebillat, F., Guette, A., Naslain, R. and Robin Brosse, C., Highly ordered pyrolytic BN obtained by LPCDV. *Journal of the European Ceramic Society*, 1997, **17**(12), 1403–1414.
12. Rebillat, F., Guette, A., Robin-Brosse, C. and Naslain, R., Chemical and mechanical alterations of SiC Nicalon fiber properties during the CVD/CVI process of boron nitride. *Acta. Metall. et Mater.*, in press.
13. Dugne, O., Prouhet, S., Guette, A., Naslain, R., and Sevely, J., Interface characterization by transmission electron microscopy and Auger electron spectroscopy in tough SiC–fiber (Nicalon)–SiC matrix composite with a boron nitride interphase. In *Developments in the Science and Technology of Composite Materials. Proceedings of ECCM3*, ed. A. R. Bunsell P. Lamicq and A. Massiah, Elsevier Applied Science, London and New York, 1989, pp 129–135.
14. Chollon, G., Pailler, R., Naslain, R., Laannani, F., Monthioux, M. and Olry, P., Thermal stability of a PCS-derived SiC fiber with a low oxygen content (Hi-Nicalon). *J. of Materials Sci.*, 1997, **32**, 327–347.
15. Chollon, G., Pailler, R., Naslain, R. and Olry, P., Correlation between microstructure and mechanical behavior at high temperature of a SiC fiber with a low oxygen content (Hi-Nicalon). *J. of Materials Sci.*, 1997, **32**, 1133–1147.
16. Rozenberg, A. S., Sinenko, Y. A. and Cherkanov, N. V., Regularities of pyrolytic boron nitride coating formation on a graphite matrix. *J. Mat. Sci.*, 1993, **28**(20), 5528–5533.

17. Thomas, J., Weston, N. E. and O'Connor, T. E., Turbostratic boron nitride thermal transformation to ordered-layer lattice boron nitride. *J. Am. Chem. Soc.*, 1963, **84**(24), 4619–4622.
18. Prouhet, S., Vignoles, G., Langlais, F., Guette, A. and Naslain, R., On the kinetics of boron nitride CVD from BF_3–NH_3–Ar: 2—Influence of the precursor composition and chemical mecanisms. *European Journal of Solid State and Inorganic Chemistry*, 1993, **30**, 971–989.
19. Leparoux, M., Elaboration à partir de la phase gazeuse des interphases BN et BNSi pour composites SiC/BN(Si)/SiC, structure et propiétés des matériaux obtenus. Ph.D. thesis, University of Orléans, France, 1995.
20. Villeneuve, J. F., Mocaer, D., Pailler, R., Naslain, R. and Olry, P., Tensile testing at high temperatures of ex-PCS Si–C–O and Si–C–N single filaments. *J. Mater. Sci.*, 1993, **28**, 1227–1236.
21. Lamon, J., Rechiniac, C., Lissart, N. and Corne, P. Determination of interfacial properties in ceramic matrix composites using microcomposite specimen *Proc. Fifth European Conference on Composite Materials (ECCM5)*, ed A. R. Bunsell, J. F. Jamet and A. Massiah. EACM, Bordeaux, 1992, pp. 895–900.
22. Corne, P., Rechiniac, C. and Lamon, J., Approche des propriétés de l'interface fibre-matrice dans les composites à matrice céramique: résistance à la décohésion. *Proc. JNC 8*, ed O. Allix, J. P. Favre and P. Ladeveze. AMAC, Paris, Nov. 1992, pp. 213–223.
23. Rebillat, F., Evans, A. and Lamon, J., Assessment of a microcomposite test procedure for evaluating constituent properties of ceramic matrix composites. *J. Am. Ceram. Soc.*, 1995, **78**(2), 401–405.
24. Weibull, W., A statistical theory of the strength of materials. Ingeniors-svetenskap Akameins, Handlinger 151, 1939.
25. Weibull, W., A statistical distribution of wide applicability. *Journal of Applied Mechanics* 1951, **51**, 293–297.
26. Lebrun, G. A. and Lamon, J., Influence de la distribution spatiale des fibres au sein d'un minicomposite sur le comportement mécanique en traction. In *Annales des Composites, 1995/4*, AMAC, 1995, pp. 121–130.
27. Jacques, S., Guette, A., Langlais, F., Naslain, R. and Goujard, S., High temperature lifetime in air of SiC/C(B)/SiC microcomposites prepared by LPCVD. *Ceramic Transactions*, 1995, **57**, 311–316.
28. Rebillat, F., Lamon, J., Guette, A. and Naslain, R., Interfacial characterization of SiC/BN/SiC composites through tensile tests on microcomposites and on 2D composites and through single fiber push-out tests. *Journal of the European Ceramic Society*, submitted for publication.
29. Jacques, S., Guette, A., Langlais, F. and Bourrat, X., Characterization of SiC/C(B)/SiC microcomposites by transmission electron microscopy. *J. of Materials Sci.*, 1997, **32**, 2969–2975.
30. Jacques, S., Guette, A., Langlais, F. and Naslain, R., Preparation and characterization of SiC/SiC microcomposites with composites with composition graded C(B) interphases. In *Key Engineering Materials*, ed. M. Fuentes, J. M. Martinez Esnaola and A. M. Dorniel, Vols 127–131, Trans. Tech. Publications, Switzerland, 1997, pp. 543–550.
31. Bertrand, S., Pailler, R., Lamon, J. and Bourrat, X., Matériaux composites céramiques SiC/SiC à interphases multicouches nanosequencées (PyC/SiC)n. Congrés de la Société Française de Chimie 1997, Bordeaux Talence, 8–11 September 1997.
32. Coffer, C. G. and Economy, J., Oxidation and hydrolitic stability of boron nitride. A new approach to improving the oxidation resistance carbonaceous structure. Carbon, 1995, **33**(4), 389–395.
33. Mieskowski, D. M., Mitchell, T. E. and Heuer, A. H., Bulle formation in oxide scales on SiC. *Com. of Amer. Ceram. Soc.*, 1984, January, 17–18.
34. Tsapuk, A. K., Polobeda, L. G. and Kovalevskii, N. N., Oxidation of materials based boron nitride, translated from *Porohkovayce Mettalurgica*, 1976, **9**, 44–47. Translation In *Test Methods and Properties of Materials*. Plessum Publishing Corporation, 1978, **3**(1–3) 51–54.